P-ISSN: 2798-1134 | E-ISSN: 2797-3549 | DOI: 10.52562/injoes.2023.800

Indonesian Journal of Earth Sciences

http://journal.moripublishing.com/index.php/injoes

| Research Article |

Analysis of Vertical Deformation and Potential Formation of New Faults Cause by Earthquake Using the DInSAR Method (Case Study: 2022 Cianjur Earthquake)

Demi Stevany*, Adi Wibowo

Department of Geography, University of Indonesia, Depok 16424, Indonesia
**Correspondence: demi.stevany21@ui.ac.id*

Received: 08 August 2023 / Accepted: 25 September 2023 / Published: 04 October 2023

Abstract: In this study, we focus on the repetitive nature of earthquakes along known fault lines and their potential to create new fault segments. Our primary aim is to enhance our understanding of fault patterns and distribution, facilitating more efficient and accurate earthquake disaster mitigation efforts. Our research specifically targets the vertical deformation resulting from the 2022 Cianjur Earthquake. To achieve this, we employed a sophisticated technique involving data processing from the Sentinel 1A satellites using the Differential Interferometric Synthetic Aperture Radar (DInSAR) method. This method allowed us to derive earthquake-induced displacement values in meters with an impressive level of accuracy, down to the centimeter scale. Our analysis revealed a conspicuous fringe pattern in the interferogram phase data, which did not align with the nearby Cimandiri Fault. This discrepancy led us to suspect the emergence of a new fault or fault segment. By comparing Sentinel 1A satellite images before and after the earthquake, we observed phase differences ranging from -3.112 to 3.117 phases. These recurring phase differences clustered at coordinates 6°48'48" South Latitude and 107°06'05" East Longitude, pinpointing the epicenter of the Cianjur earthquake on November 21, 2022. Furthermore, we calculated line-of-sight (LoS) displacement values ranging from 0 to minus 102 millimeters, indicating vertical subsidence in the vicinity of the 2022 Cianjur earthquake. In conclusion, our research underscores the utility of the DInSAR method for assessing Earth's surface deformation patterns, making it a valuable tool for various earthquake-related analyses.

Keywords: DInSAR, Synthetic Aperture Radar, Earthquake, Cianjur

INTRODUCTION

Earthquakes manifest as ground vibrations resulting from the sudden release of energy, which subsequently propagates in all directions from the epicenter (Lutgens et al., 2015). In the context of Indonesia, earthquakes are notably frequent and intense due to the convergence of three tectonic plates, creating pathways for both seismic activity and volcanic eruptions, significantly influencing the distribution of earthquakes in the region (Kurniawan et al., 1997). Beyond tectonic forces, earthquakes can stem from various sources, including meteor impacts, volcanic events, landslides, mining-related activities, and even underground nuclear detonations (Boen, 1995).

To advance our comprehension of earthquakes and bolster our preparedness and mitigation strategies, fundamental research into their potential and underlying physical processes is imperative. Moreover, there is a pressing need for the development of robust information systems for real-time earthquake monitoring and post-event communication (BNPB, 2019). In this study, we employ the Differential Interferometric Synthetic Aperture Radar (DInSAR) method, a technique combining physical and mathematical modeling to spatially describe earthquake-induced deformations, encompassing patterns and distribution. This approach allows for a precise assessment of earthquake hazards and potential risks.

Faults, structural features formed by tectonic movements, play a pivotal role in seismological activity (Dong & Luo, 2022). They arise from the deformation of rock layers under the influence of tensile and shock forces associated with crustal movements. Fault structures are intricately tied to seismological phenomena (Li et al., 2019). The strength of faults results from the interaction of low-friction minerals, such as phyllosilicates, and high pore fluid pressures, leading to the formation of a network of weak faults amidst adjacent robust rock formations. However, identifying regions of new

fault development and the sequence of fault formation events remains challenging, leaving the initiation mechanism unresolved (Copley, 2018). Thus, this study employs radar-based methods to mathematically and spatially elucidate crustal deformations.

In fault zones, earthquakes stemming from the gradual deformation of tectonic plates give rise to surface alterations. Interseismic deformation, occurring between seismic events at relatively long intervals, reflects steady movements deep within the crustal blocks flanking the fault. These blocks, driven by tectonic forces, exhibit continuous motion, causing the upper crust to twist in response. The nature of this deformation informs us about the extent and rate of crustal movement. Notably, satellite geodetic measurements have consistently shown concentrated strain along major strike-slip fault zones during the interseismic period, a significant discovery (Wright et al., 2013).

Our case study focuses on the Cianjur earthquake of November 21, 2022, at 13:21:10 WIB. According to the Indonesian Meteorological, Climatological and Geophysical Agency (BMKG), the earthquake's epicenter was situated at coordinates 6.84 LS – 107.05 with a depth of 11 km and a magnitude of 5.6. Subsequently, as of November 28, 2022, at 07:00 WIB, the BMKG recorded 297 aftershocks, ranging from a substantial magnitude of M4.2 to as small as M1.0. According to the Indonesian Center of Volcanology and Geological Hazard Mitigation (PVMBG) (2022), the magnitude of the main earthquake did not result in surface rupture. Nevertheless, the rupture area, indicating the region of fault movement, could be estimated based on the convergence of the epicenter and aftershocks. This area extends approximately 12 km in a southwest-northeast direction, from Warungkondang to Karang Tengah, covering an area of about 8 km in width. Consequently, Figure 1 illustrates the research location in the vicinity of the 2022 Cianjur earthquake's epicenter, marked by a red star in line with information from the 2022 BMKG.

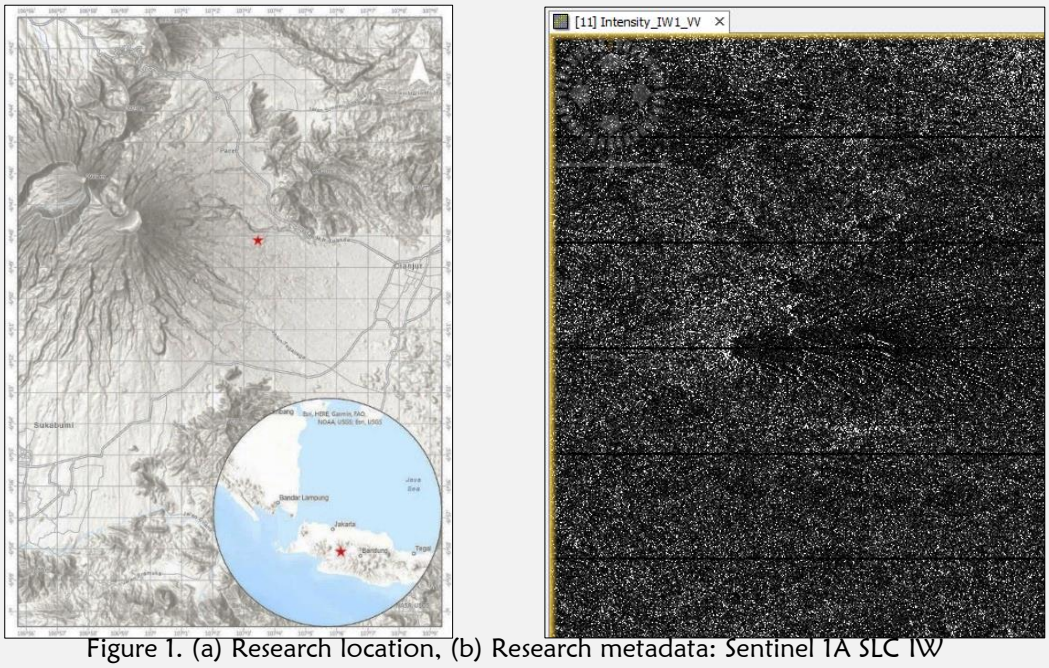

Figure 1. (a) Research location, (b) Research metadata: Sentinel 1A SLC IW

The decision to employ the DInSAR technique in our study was influenced by the earthquake's relatively modest magnitude, which didn't result in surface faulting. This approach allows us to model earthquake-induced deformations, including the potential identification of new faults, as we will discuss in the results section. Utilizing DInSAR observations addresses the scarcity of spatial data, especially in areas susceptible to earthquakes, which could exacerbate potential losses. Cianjur Regency, as per BNPB data, experienced a destructive earthquake in 2009 (Kusmajaya & Wulandari, 2019). Recognizing and understanding potential hazards in our surroundings constitute the initial steps toward disaster risk reduction. Hence, this research provides an overview of deformation hazards arising from earthquakes.

Aligned with the principles and commitments of sustainable global development, the 2016 New Urban Agenda (NUA) explicitly emphasizes disaster risk reduction (DRR) and resilience. It advocates for

a proactive, risk-based approach to society, promoting sustainable natural resource management in urban areas to enhance DRR through the development of strategies and regular disaster risk assessments. Furthermore, the NUA underscores member countries' commitment to enhancing urban resilience to disasters in line with the Sendai Framework (UN, 2015).

Therefore, research on earthquake-induced deformations holds significant value in mapping the size and extent of areas at risk, aiding in the analysis of potential risks. This information can be instrumental in devising appropriate mitigation measures and strategies to reduce earthquake-related risks, particularly for Indonesia and other nations situated in the volatile "Ring of Fire" region.

METHOD

This research was undertaken to investigate the spatial deformations resulting from the 2022 Cianjur earthquake. The analysis focused on quantifying the extent of deformation along the active fault segment, utilizing Sentinel imagery for this purpose. The Sentinel data was collected both before and after the earthquake that occurred on Monday, November 21, 2022, at 13:21 WIB, registering a magnitude of 5.6 on the Richter scale. On the same day, there were 15 aftershocks, with a maximum magnitude of M4.0. According to information from the Meteorology, Climatology and Geophysics Agency (BMKG), the earthquake's epicenter was situated on land at coordinates 107.05 East Longitude and 6.84 South Latitude, approximately 9.65 km southwest of Cianjur City or 16.8 km northeast of Sukabumi City.

The data utilized in this analysis comprises level-1 data from Sentinel 1 A, featuring Single Look Complex (SLC) products with spatial resolutions dependent on the acquisition mode. We opted for the Interferometric Wide Swath Mode (IW) as our acquisition mode due to its implementation of TOPSAR, a variant of ScanSAR imaging. In TOPSAR, the radar beam is cyclically switched among three sub-swaths, with one azimuth look per beam for all points. The satellite is equipped with a C-SAR instrument, featuring an active phased array antenna designed to enable rapid scanning in various elevations and azimuths. It operates at a frequency of 5.041 GHz, with a central wavelength of 6 cm and a half-wavelength of 3 cm. For polarization, we employed VV polarization, signifying Vertical polarization on transmit and Vertical polarization on receive. You can find detailed specifications of the Sentinel 1 A data used in the case study in Table 1.

Table 1. Sentinel used in research

No.	Sentinel 1	Acquisition	Track	Orbit
1	S1A_IW_SLC__1SDV_20221201T223409	19Nov2022	47	45969
2	S1A_IW_SLC__1SDV_20221119T223410	1Dec2022	47	46144

The methodology employed in this study to model earthquake-induced deformation is Differential Interferometry Synthetic Aperture Radar (DInSAR), which calculates the phase difference between two Synthetic Aperture Radar (SAR) images acquired on the same orbit. The DInSAR processing was conducted using SNAP software. The specific steps of this process are detailed in Figure 2, assuming a dataset of Sentinel-1A SLC IW SAR images was collected at specific times (before and after the earthquake) covering the study area.

The initial step involves generating and combining the SLC IW imagery with external DEM (Digital Elevation Model) data, specifically the SRTM HGT 1 dataset, along with precise orbit information. The interferogram is generated with constraints on perpendicular and temporal baselines, and the DEM data is used to correct for topographical effects. Subsequently, adaptive filtering and unwrapping phases are applied to obtain an unwrapped differential interferogram dataset. Following this, a simple linear model is utilized to remove topography-dependent atmospheric phases, which can be expressed in the formula (Xu et al., 2022):

$$\phi diff = \phi def + \phi topo_{res} + \phi atm\_res + \phi noise \quad (1)$$

The deformation phase comprises several components, including topography-related effects, atmospheric artifacts, decorrelation, thermal noise, and ground deformation along the Line of Sight (LoS) of the radar. Once the other phase components have been subtracted, the remaining unwrapped differential interferometric phase represents the deformation phase, which can subsequently be converted into displacement, providing the DInSAR results.

In DInSAR, the phase difference is computed by comparing the two SAR images pixel by pixel, resulting in an interferogram that depicts phase differences. These phase differences correspond to variations in the SAR signals caused by deformation. It's worth noting that the values in the interferogram typically range from 0 to 2π or one wavelength cycle, determined by the specific sensor's characteristics (Crosetto, 2002).

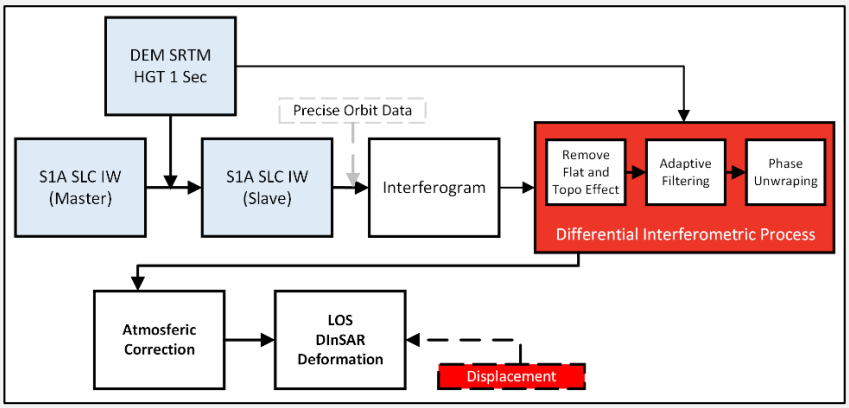

Figure 2. Research Scheme.

Following the interferogram process, we encounter overlapping information in each burst, both in the range and azimuth directions. This overlap is essential for achieving continuous ground coverage. Up to this point, each burst has been processed as an individual SLC image. To seamlessly merge these bursts, particularly in the azimuth direction, and retain the phase information, we employ a merging procedure. Additionally, in the overlapping range region, merging is performed between subswaths. To facilitate this, we implement Topographic Phase Removal, which estimates and subtracts the topographic phase from the deburst interferogram.

Subsequently, we carry out a "Multilooking" process to mitigate the inherent speckle noise that initially appears in SAR images, resulting in the acquisition of square pixels. This step enhances the quality of the data.

Phase filtering is the subsequent operation, aimed at reducing phase noise. This phase filtering is crucial as it significantly improves the accuracy of the phase unwrapping process in subsequent stages.

At this juncture, we obtain coherence information by interfering the two images through InSAR (Interferometric Synthetic Aperture Radar). Coherence values typically range from 0 to 1, representing the quality of the interference. A higher coherence value closer to 1 signifies a stronger deformation signal and provides insights into the magnitude of deformation. Figure 3 showed the Coherence value information.

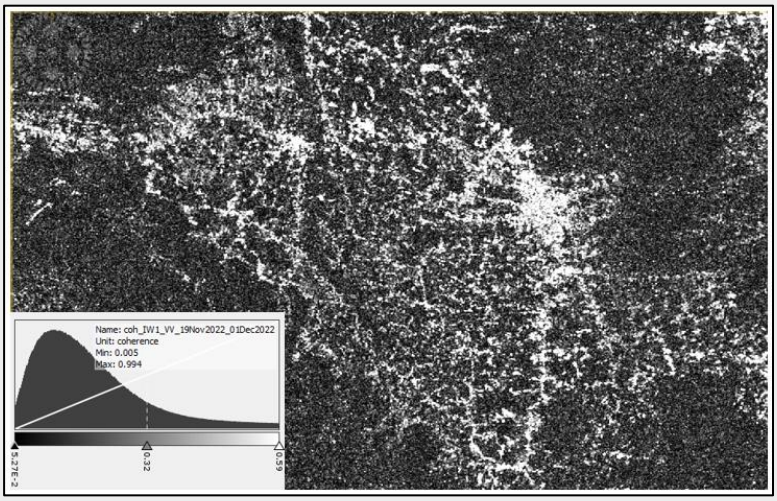

Figure 3. Coherence value information with a value of 0.005-0.994.

After obtaining the coherence information, the next crucial step in the process is phase unwrapping. Phase unwrapping is necessary to convert phase units into length units. It involves recovering unambiguous phase data from a 2-D array of phase values that are known only modulo 2π radians. These unwrapped phase results are then converted into displacements, allowing us to quantify ground movements accurately.

Following phase unwrapping, Terrain Correction is applied to the product containing the unwrapped interferogram and the one containing the displacement. This correction process transforms the RADAR coordinates into geographic coordinates, ensuring that the final results are in a format suitable for geographic analysis.

The primary product of this study is the difference in SAR phases between the master image acquired on November 21, 2022, and the slave image acquired on December 1, 2022. These image pairs cover both the main shock and aftershock of the 2022 Cianjur earthquake. This phase difference is further processed by adding and comparing it with other variables and parameters relevant to the study. Table 2 summarize the data used in the research.

Table 2. Data used in research

No.	Data	Format	Source
1	Sentinel I A SLC IW	Raster	ESA
2	Sukabumi Earthquake Epicenter Data	Vektor	BMKG
3	Indonesian Fault Data	Vektor	BMKG

Regarding prior research, this study builds upon effective methods and analyses employed in previous studies of earthquake deformation. The methodology used in this research is the DInSAR technique (Mabaquiao, 2021), focusing on displacement analysis between two SLC Sentinel images (Mohammadi et al., 2020). The SRTM high verification technique is utilized for topographical phase removal (Priya & Pandey, 2021). The initial outcome of this processing is the Line of Sight (LoS) displacement (Bayik, 2021). While the DInSAR method is well-suited for monitoring nonlinear deformation, it may not be ideal for long-term deformation monitoring. To explore potential errors other than spatiotemporal incoherence in DInSAR results, two images with a time baseline of 12 days and a spatial baseline of 9 meters were selected for DInSAR processing (Xu et al., 2022).

RESULTS

Results of this study can be categorized into two sub-results: the interferogram phase results and the displacement results.

Interferogram Phase Results

The phase data analysis yielded phase difference values ranging from -3.112 to 3.117 phases. Areas experiencing deformation are indicated by repeating phases that form lines, often referred to as fringes. In particular, the presence of numerous and densely packed phase differences (fringes) is observed at coordinates 6°48'48" LS and 107°06'05" E. These fringes serve as markers identifying the location of the epicenter of the Cianjur earthquake on November 21, 2022, as depicted in Figures 4(a) and (b). If a cross-sectional line is drawn across these fringes (as shown in Figure 4(b)), it reveals a graphic plot (Figure 5) displaying significant fluctuations in phases, serving as an indication of the epicenter of the 2022 Cianjur earthquake.

Each interferometric phase represents the difference in ground distance between two satellite passes. One fringe corresponds to one cycle of spectrum colors, transitioning from purple to red. The displacement represented by a single color fringe is half the wavelength of the SAR instrument's band. To calculate the total displacement, one counts the number of color fringes and multiplies it by the scale. In this case, as observed, the fringes progress through the spectrum from red to purple, indicating that the ground has moved closer to the satellite, resulting in a negative phase change. Consequently, the gross total displacement inferred from the results of this phase interferogram is approximately 10.5 cm (105 mm) of ground subsidence, considering that one color fringe corresponds to around 3 cm (half the wavelength of band C Sentinel 1A).

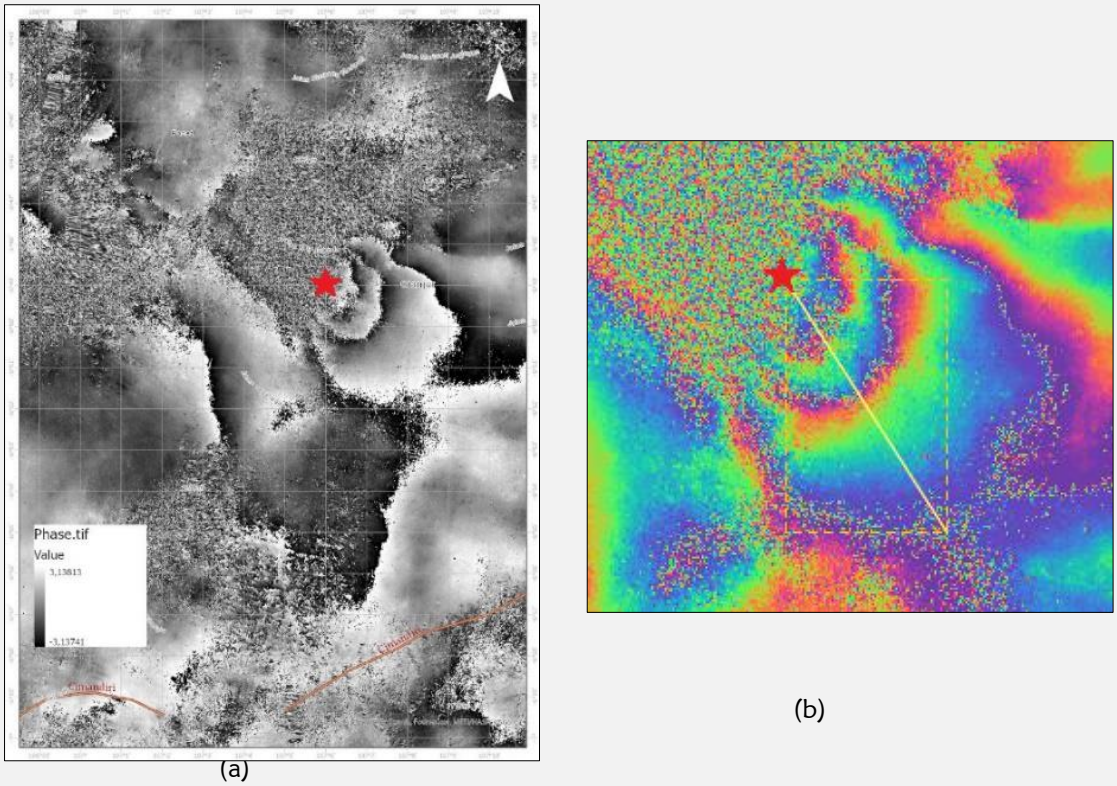

Figure 4. (a) Interferogram Phase Results, (b) Fringe Cross Section.

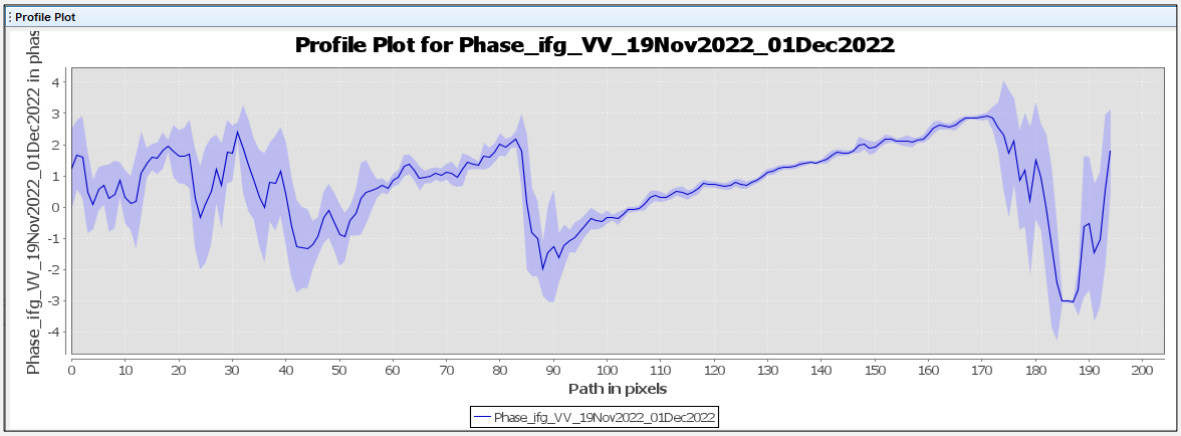

Figure 5. Profile fringe cross-section plot along the yellow transect line in Figure 4(b).

Displacement Results

The decision to employ the DInSAR technique was driven by the moderate magnitude of the earthquake, which did not result in surface faulting but did cause significant deformation. The displacement results, in terms of absolute values, along the Line of Sight (LoS), range from 0 to minus 102 millimeters. These values indicate that the area around the 2022 Cianjur earthquake, particularly in the Cugenang sub-district and its vicinity, has experienced vertical subsidence.

In examining the distribution pattern of vertical deformation, no overlapping faults were detected at the location of the known Cimandiri Fault. Instead, there are indications of the formation of new faults or fault segments. Drawing a straight line from the displacement distribution area to the nearest Cimandiri Fault area reveals a gap of approximately 15 km. The Cimandiri Fault is depicted by the southern red line symbol in Figure 6.

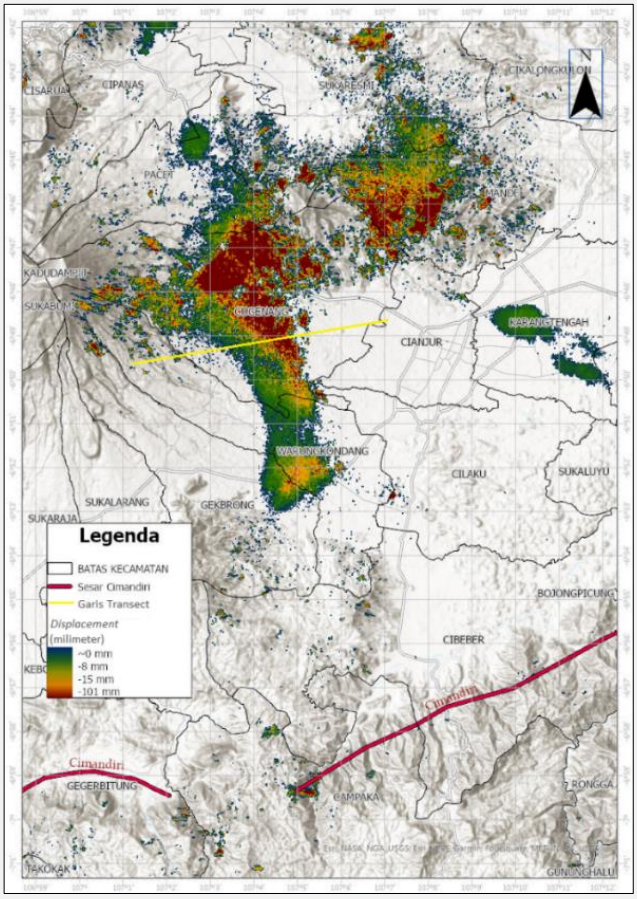

Figure 6. Displacement Result.

A cross-sectional profile plot (Figure 7) was generated along the transect line (yellow line in Figure 6). The results of this profile plot, as shown in Figure 6, reveal deformation in the form of subsidence.

It's important to note that the observation of the fringe phase interferogram necessitates the calculation of absolute values, specifically by quantifying the displacement to accurately determine the absolute displacement at each location point and its distribution. These observations make it evident that the displacement distribution does not align with the known Cimandiri Fault location, thereby strengthening the possibility of the formation of new faults in the area.

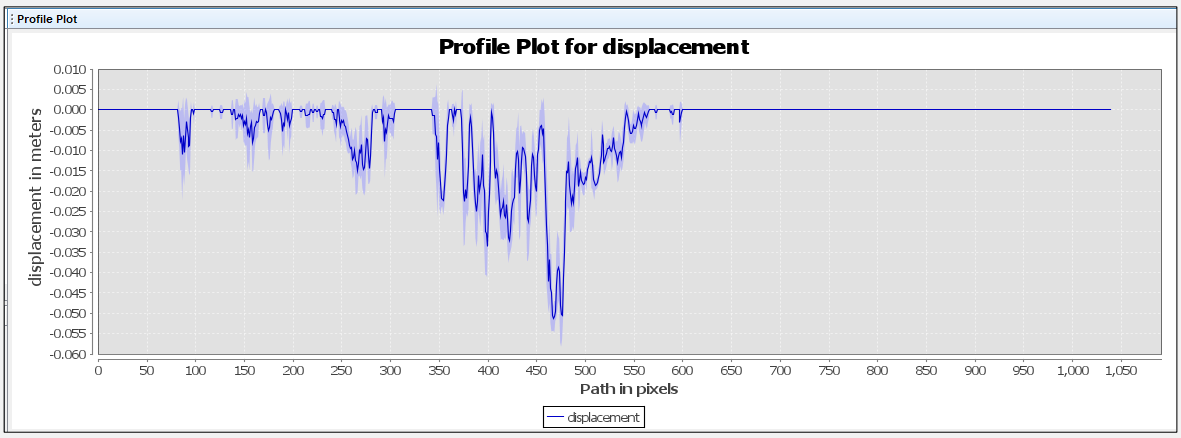

Figure 7. Vertical Profile Plot of displacement along the yellow transect line in Figure 5.

DISCUSSION

Formation of a New Fault- Cugenang Fault

This research has adopted the DInSAR technique, as previously discussed, which is commonly used for post-earthquake deformation analysis and subsidence assessment in coastal areas and cities. However, in this study, it has been observed that DInSAR results can do more than mathematically describe deformation magnitude; they can also depict the spatial distribution of new fault formations resulting from earthquakes. This discovery indicates the need for further research in this direction.

The analysis of deformation distribution caused by the 2022 Cianjur earthquake did not align with the pattern of the nearest known fault. This observation strongly suggests the formation of a new fault around the region indicated by the DInSAR results (Figure 5), with the epicenter located in the Cugenang District. The Indonesian Meteorological, Climatological, and Geophysical Agency (BMKG) confirmed during a press conference on December 12, 2022, that the trigger for the Cianjur earthquake on November 21, 2022, with a magnitude of 5.6, was indeed the Cugenang fault. This fault was identified in a survey conducted by the BMKG and stretches approximately 9 kilometers, crossing at least 9 villages. Eight of these villages belong to the Cugenang District, including Ciherang Village, Ciputri Village, Cibeureum, Nyalindung, Mangunkerta, Sarapad, Cibulakan, and Benjot Village. The remaining village, Nagrak, is located within the Cianjur District area (Putratama, 2022).

A study by Markušić et al. (2020) in Zagreb, Croatia, which was struck by an M5.5 earthquake, used Sentinel-1 interferometric wide-swath data to estimate co-seismic vertical ground displacement. This research found approximately 3 cm of uplift in the affected area. Similar to our study, they applied the differential interferometric synthetic aperture radar (DInSAR) technique. However, in our case, the displacement distribution was not aligned with the Cimandiri fault but occurred in a new location with no prior fault history. In essence, DInSAR proved capable of providing patterns and distribution of deformation locations resulting from earthquakes, whether on existing faults or in the formation of new ones.

According to Xu et al. (2022), DInSAR is a valuable Earth observation method known for its ability to measure surface deformation induced by various activities, including earthquakes. It offers advantages such as large spatial coverage, low cost, high accuracy, and all-weather observation capabilities. While it excels in nonlinear deformation monitoring, it is typically used for short-term monitoring with imaging periods ranging from weeks to months, as in our research case with a temporal resolution difference between master and slave images of 12 days.

The rapid and accurate determination of distribution and deformation patterns using DInSAR data processing techniques, with centimeter-level accuracy, can greatly support efficient analysis of new faults. Sentinel-1A satellite data is available on the same orbit every 12 days, allowing for quick detection of earthquake-induced deformation and the formation of new faults within this timeframe.

It's important to note that this research represents a contribution to better understanding the geodynamics of the new fault system in the Cianjur Area. Field validation through leveling measurements and GPS geodetic static methods is recommended for future research to obtain more precise and specific results. The authors express their willingness to share their research data for future research purposes.

CONCLUSION

The use of DInSAR as a method for earthquake monitoring has proven highly effective, providing data with both high spatial and temporal resolution. This technique has the potential to deliver timely and precise reports on the magnitude, extent, and distribution patterns of earthquakes. In the context of the 2022 Cianjur earthquake, this research has concluded that DInSAR successfully identified vertical subsidence, even though the earthquake did not result in surface faulting. The displacement results obtained through DInSAR have not only quantified the magnitude of subsidence (up to minus 101 mm) but have also outlined its distribution. This distribution is invaluable for mapping new faults or fault segments, thereby contributing to future mitigation efforts and disaster risk reduction.

The research has highlighted the potential operationalization of the DInSAR method by relevant agencies for earthquake risk mitigation and reduction. The reference to the 2030 Agenda, which specifically cites the Sendai Framework for reducing disaster risk and emphasizes an "enriched data environment for enhanced assessment capability," underscores the importance of mapping vertical deformation hazard areas as a means of enriching data and facilitating more precise and efficient decision-making.

Future work in this field should include focused geological mapping, more detailed spatial and temporal analyses of the entire seismic sequence, and an examination of the co-seismic movements

associated with the new fault identified in the geodynamic GPS network of the Cianjur Regency. These endeavors will further advance our understanding of earthquake dynamics and contribute to improved disaster risk reduction strategies.

ACKNOWLEDGMENT

The author would like to thank the Geography University of Indonesia, LPDP, the European Space Agency, BMKG, Esri Geography UI, and the Indonesian Journal of Earth Sciences for providing workspaces, data, software licenses, sponsoring, and the opportunity to publish the journal. We also thank those who cited this journal.

REFERENCES

Badan Nasional Penanggulangan Bencana. (2019). *Risiko Bencana Indonesia*.

Bayik, C. (2021). Deformation analysis of 2020 MW 5.7 Karlova, Turkey, earthquake using DInSAR method with different incidence angle SAR data. *Arabian Journal of Geosciences, 14*, 273. https://doi.org/10.1007/s12517-021-06670-x

Boen, T. (1995). *Earthquake Phenomena, a Two-day course on the earthquake-resistant design of buildings*.

Copley, A. 2018. The Strength of earthquake generating faults. *Journal of the Geological Society, 175*, 1-12. https://doi.org/10.1144/jgs2017-037

Crosetto, M. (2002). Calibration and validation of SAR interferometry for DEM generation. *ISPRS Journal of Photogrammetry and Remote Sensing, 57*(3), 213–227. https://doi.org/10.1016/s0924-2716(02)00107-7

Dong, L., & Luo, Q. (2022). Investigations and new insights on earthquake mechanics from fault slip experiments. *Earth-Science Reviews, 228*, 104019. https://doi.org/10.1016/j.earscirev.2022.104019

European Space Agency. (n.d.). *Level-1 Single Look Complex. User Guides*. ESA.

Kurniawan, L., Naryanto, H. S., & Santoso, E. W. (2007). Pasca Gempa Kerinci Tahun 1995 dan Rencana Kontigensi (Contingency Planning). *Alami: Jurnal Teknologi Reduksi Risiko Bencana, 2*(3), 32-35.

Kusmajaya, S., & Wulandari, R. (2019). Kajian risiko bencana gempabumi di kabupaten cianjur. *Jurnal Dialog dan Penanggulangan Bencana, 10*(1), 39-51.

Li, P., Ren, F., Cai, M., Guo, Q., & Miao, S. (2019). Present-day stress state and fault stability analysis in the capital area of China constrained by in situ stress measurements and focal mechanism solutions. *Journal of Asian Earth Sciences, 185*, 104007. https://doi.org/10.1016/j.jseaes.2019.104007

Lutgens, F. K., Tarbuck, E. J., & Tasa, D. (2015). *Essentials of geology*. Boston, MA, USA: Pearson.

Mabaquiao, L. C. (2021). InSAR-Based LOS Surface Deformation Comparison of Metro Manila Before and after the January 2020 Taal Volcano Eruption. *The International Archives of the Photogrammetry, Remote Sensing and Spatial Information Sciences, 46*, 201-206. https://doi.org/10.5194/isprs-archives-XLVI-4-W6-2021-201-2021

Markušić, S., Stanko, D., Korbar, T., Belić, N., Penava, D., & Kordić, B. (2020). The Zagreb (Croatia) M5. 5 Earthquake on 22 March 2020. Geosciences, 10(7), 252. https://doi.org/10.3390/geosciences10070252

Mohammadi, A., Karimzadeh, S., Valizadeh Kamran, K., & Matsuoka, M. (2020). Extraction of land information, future landscape changes and seismic hazard assessment: A case study of Tabriz, Iran. *Sensors, 20*(24), 7010. https://doi.org/10.3390/s20247010

Priya, T., & Pandey, A. C. (2021). Geoinformatics-based assessment of land deformation and damage zonation for Gorkha earthquake, 2015, using SAR interferometry and ANN approach. *SN Applied Sciences, 3*, 573. https://doi.org/10.1007/s42452-021-04574-9

Putratama, R. (2022). *Gempa Cianjur Disebabkan Sesar Cugenang, BMKG Dorong Pemkab Cianjur Relokasi 9 Desa*. Retrieved from https://www.bmkg.go.id/berita/?p=gempa-cianjur-disebabkan-sesar-cugenang-bmkg-dorong-pemkab-cianjur-relokasi-9-desa&lang=ID

United Nations. (2015). *Global Assessment Report on Disaster Risk Reduction 2016*. United Nations Office for Disaster Risk Reduction.

Wright, T. J., Elliott, J. R., Wang, H., & Ryder, I. (2013). Earthquake cycle deformation and the Moho: Implications for the rheology of continental lithosphere. *Tectonophysics, 609*, 504-523. https://doi.org/10.1016/j.tecto.2013.07.029

Xu, Y., Li, T., Tang, X., Zhang, X., Fan, H., & Wang, Y. (2022). Research on the Applicability of DInSAR, Stacking-InSAR, and SBAS-InSAR for Mining Region Subsidence Detection in the Datong Coalfield. *Remote Sensing, 14*(14), 3314. https://doi.org/10.3390/rs14143314